



## TESTS ON THE LOAD BEARING BEHAVIOUR OF MASONRY SHEAR WALLS

**U. Schmidt<sup>1</sup>, I. Beer<sup>2</sup> and W. Brameshuber<sup>3</sup>**

<sup>1</sup>Dipl.-Ing. Ulf Schmidt, Scientific employee and head of the working group “masonry” at the Institute of Building Materials Research, RWTH Aachen University

<sup>2</sup>Dipl.-Ing. Ingo Beer, Scientific employee at the Institute of Building Materials Research, RWTH Aachen University

<sup>3</sup>Professor Dr.-Ing Wolfgang Brameshuber, Director of the Institute of Building Materials Research, RWTH Aachen University

### ABSTRACT

Evaluations of test results on the shear load bearing capacity of masonry have shown that in some cases clearly marked deviations exist between experimental test results and calculation formulae which are the basis of the design code in Germany. Within the scope of a research project carried out at the Institute of Building Materials Research, tests and numerical simulations were performed on the shear load bearing behaviour of masonry walls. In a large number of small-scale specimen tests the material laws for masonry units and the bonding properties between masonry unit and mortar were determined, in some cases inversely by Finite-Element-Calculation of the small-scale specimen tests. The experimental tests carried out on storey-high masonry walls of autoclaved aerated concrete, in which the inhomogeneity of the masonry was raised incrementally, were simulated with the Finite-Element-Method. The results of the experimental tests and the simulations are in good conformity.

**KEYWORDS:** shear load bearing capacity, autoclaved aerated concrete, material laws, finite-element-calculations

### INTRODUCTION, STATE OF THE ART

Masonry building components are subjected to stress from compression, bending or shear forces according to their respective functions. Masonry walls subjected to shear stresses are generally stiffening masonry walls, which are under load resulting from earth pressure, wind, and also earthquakes. Proof of the adequate shear load bearing capacity can be given in Germany according to German Standard DIN 1053-1 [1] or the Eurocode 6 [2] with reference to the National Application Document. The basic principles of the shear design equations both in [1] and [2] come from theoretical considerations developed in the 1970s by *Mann and Müller* [3, 4, 5], which were verified on masonry test specimens of small-size solid masonry units (model masonry). Through theoretical consideration of the individual masonry unit, four failure criteria were derived, one of which may govern according to the building material properties and stress applied. It was assumed that no shear stresses can be transferred through the head joints and that

to maintain force equilibrium against distortion of the masonry units, non-uniform compressive stresses are effective, vertical to the bed joint. A distinction is made between:

- Opening of the bed joint (failure of the tensile bond strength between the masonry unit and the mortar)
- Failure of the bed joint in shear (friction failure)
- Failure of the masonry unit due to exceeding the masonry unit tensile strength as a result of the main stresses
- Exceeding the masonry compressive strength.

The calculation formulae given in [3, 4, 5] were further developed by various authors. In [6] the model from [3, 4, 5] was extended to such a degree that shear stresses are also transferred in the head joints. Both models and the Finite-Element-Modellings presented in [7] form the basis for the calculation formulae described in [8, 9]. Essential innovations by *Simon and Graubner* are consideration of the overlap and the analytical description of the additional failure criterion “Exceeding the masonry unit tensile strength at the edge of the masonry unit”. Experimental tests and numerical calculations were not carried out in [8, 9]. The above extended model formulae, and others, have been published in brief summary form in [10].

Evaluations in [10] have shown that definite differences exist between experimental test results and calculated values from formulae in the current design specifications. Thus, the aim of a research project carried out at the Institute of Building Materials Research, RWTH Aachen University, which was began approximately the same time as the theoretical investigations of *Simon and Graubner*, was to determine systematically the states of stress in masonry under shear load with the help of experimental tests and numerical simulations. For this purpose characteristic values of specific geometrical and material parameters of importance should be investigated more completely and exactly.

## **TEST PROGRAMME**

The experimental tests and numerical calculations were carried out on storey-high, square masonry panels (2.50 m). In these “isotropic” masonry panels, solid units with mortared head joints were tested first. The inhomogeneity of the masonry was gradually increased by incorporating non-mortared head joints and varying the overlap. For all the tests the same masonry unit material – autoclaved aerated concrete units of class 4 compressive strength – were used without a handling device and without a tongue-and-groove system, see Figure 1 left. For the masonry unit material, the same material laws were applied in every case and thus the geometrical variables could be deliberately tested. By using autoclaved aerated concrete units it was also possible to produce vertically perforated units from the same masonry unit material but no longer with isotropic properties, and thus increase the inhomogeneity of the masonry further. Such a vertically perforated masonry unit is shown on the right of Figure 1.

A thin-layer mortar and a general purpose mortar were used to construct the masonry panels. The combination of autoclaved aerated concrete units with general purpose mortar is not usual or relevant in practice. However, the relevant failure criteria could be tested both in the case of joint failure and also of masonry unit failure with the selected masonry units of one strength class. An essential part of the research project consisted of tests on small specimens to determine the required material laws of the autoclaved aerated concrete units and the bonding properties of

masonry units and mortar for the numerical simulation of the wall tests. For this, an independent comparison of the numerical simulation of the wall tests with the experimental results – without adaptation of the material properties for better conformity – is possible.



**Figure 1 – The masonry units used  
(length · width · height = 499 · 300 · 249 mm<sup>3</sup>)**

### **EXPERIMENTAL TESTS ON SMALL TEST SPECIMENS**

Tests on small test specimens were carried out to determine the material laws of the masonry unit material and also the bonding properties between the masonry units and masonry mortar. In some cases the material laws could be directly determined from the experimental tests, whereas in other cases an inverse determination of the material laws was made by numerical simulation of the small test specimen results. The tests carried out on the small test specimens and their results are presented below.

#### **(1) Compressive strength and load deformation behaviour under compressive stress**

The standardised compressive strength of the high precision autoclaved aerated concrete masonry units was determined in the same way as in [11] on cubes and on entire masonry units. For the determination of the load deformation behaviour of the autoclaved aerated concrete material and for the derivation of material laws, tests were carried out on slender autoclaved aerated concrete prisms and cylinders, so that the influence of platen restraint was minimized. On the test specimens the axial and lateral deformations were determined with linear variable displacement transducers (LVDT) or an extensometer chain (circumferential extensometer). A test specimen for the determination of the compressive strength is illustrated in Figure 2 (left). Figure 2 (right) shows the stress-strain curves determined. The results of the compressive strength tests are summarized in Table 1.

**Table 1 – Properties of the masonry units (compression tests)**

|  | Cube <sup>1)</sup> | Solid unit <sup>1)</sup> | Perforated unit <sup>1)</sup> | Prism | Cylinder |
|--|--------------------|--------------------------|-------------------------------|-------|----------|
| Compressive strength [N/mm <sup>2</sup> ]              | 4.0                | 4.0                      | 3.4                           | 3.9   | 3.7      |
| Compressive modulus of elasticity [N/mm <sup>2</sup> ] | -                  | -                        | -                             | 1784  | 1893     |
| „Poisson's ratio“ [-]                                  |                    |                          |                               | 0.11  | 0.14     |

1) Without application of the shape factors according to [11]

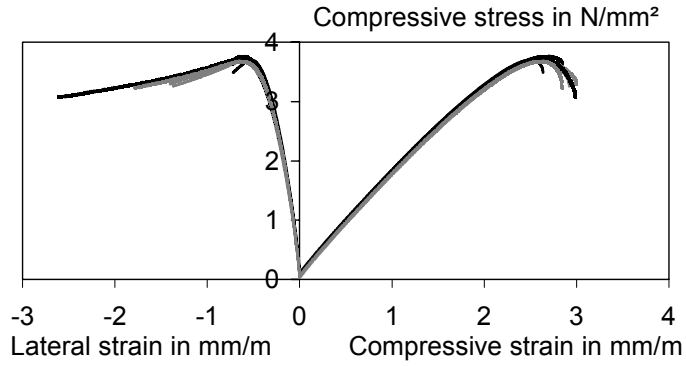


**Figure 2 – Compression tests on autoclaved aerated concrete cylinders**

**(2) Tensile strength and load deformation behaviour under tensile stress**

For the description of the load deformation behaviour under tensile load, cylinders with a diameter of 100 mm were cored from the high precision autoclaved aerated concrete units in the directions of unit height and unit length. Then, from these specimens, the test specimens shown in Figure 3 (left) were milled with a tapered cross-section. Load application was made by steel plates attached and flexibly joined to the testing machine and glued onto the test specimens. The load-dependent deformations were determined with linear variable displacement transducers (LVDT). The specific stress-strain curves are illustrated in Figure 3 (right).

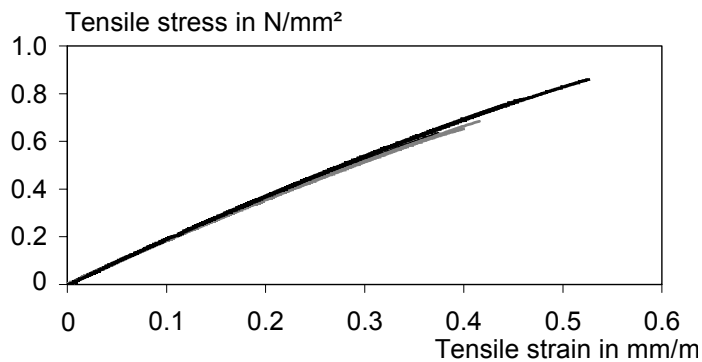
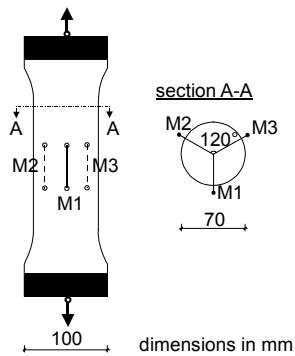


**Figure 3 – Tensile tests on autoclaved aerated concrete cylinders**

In addition, the tensile strength was determined on the solid and perforated masonry units shown in Figure 1, both in the direction of unit length and also in that of unit height. The test results are given in Table 2.

**Table 2 – Properties of the masonry units (axial tensile tests)**

|   | Cylinder    |             | Solid masonry unit |             | Vertically perforated masonry unit |             |
|---|-------------|-------------|--------------------|-------------|------------------------------------|-------------|
|   | unit-height | unit-length | unit-height        | unit-length | unit-height                        | unit-length |
| Tensile strength [N/mm <sup>2</sup> ]                                       | 0.72        | 0.52        | 0.45               | 0.35        | 0.29                               | 0.19        |
| Secant tensile modulus of elasticity (E <sub>S</sub> ) [N/mm <sup>2</sup> ] | 1847        | 1866        | 2182               | 1877        | 1854                               | 1365        |

### (3) Bending tensile strength, fracture mechanical characteristic values

In order to determine the post-peak behaviour of the autoclaved aerated concrete under tensile stress, deformation-controlled 3-point bending tests (span 400 mm) were carried out on notched and unnotched autoclaved aerated concrete prisms ( $500 \cdot 100 \cdot 100 \text{ mm}^3$ ) taken in the direction of the masonry unit length. The test equipment, which allows compensation for the specimen's own weight, is presented in Figure 4 (left). The load deflection curves determined on prisms with a notch depth of 50 mm are shown in Figure 4 (right).

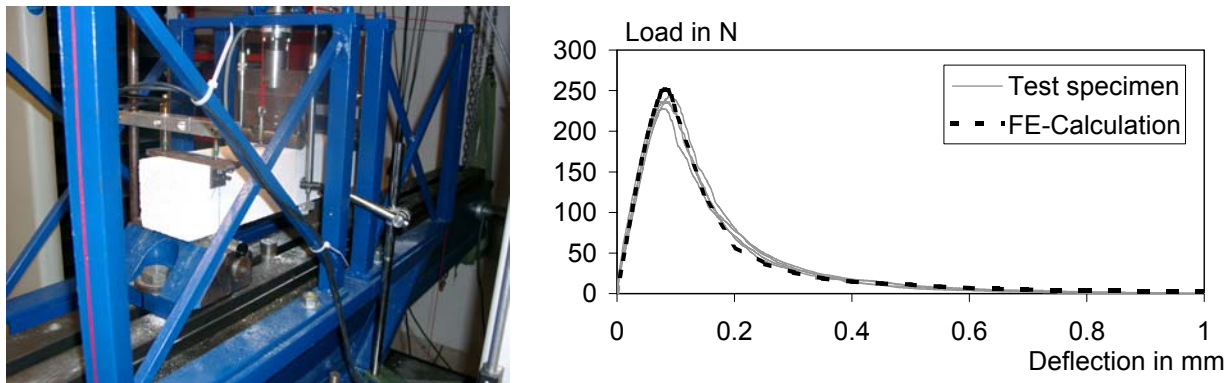


**Figure 4 – Test equipment for the determination of the bending tensile strength and comparison of the experimental load-deflection curves with results from Finite Element calculations**

The bending tests were simulated with the Finite-Element-Method. By variation of the stress-crack opening relation (tensile strength  $f_t$ , calculated tensile modulus of elasticity  $E_{cal}$ , fracture energy  $G_F$ ) in the numerical simulation, the load-deflection curves were adapted as well as possible to the experimental test results (Figure 4 (right)). Thus the material law of the autoclaved aerated concrete material, necessary for the calculation of the wall tests, was determined inversely. The result of the inverse calculation of the material model law is shown in Figure 5.

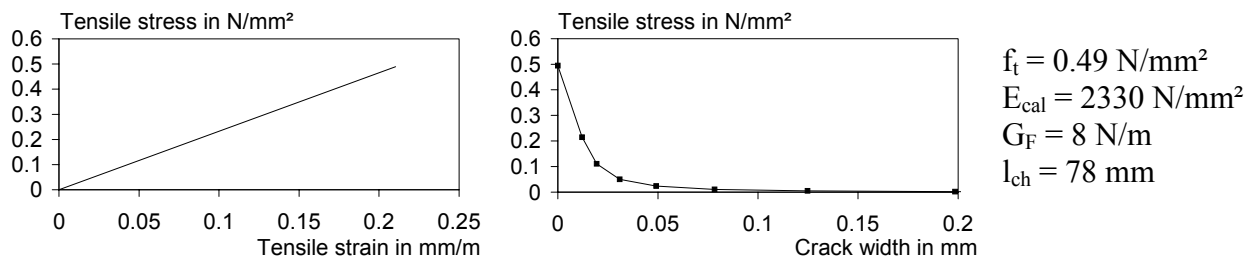


**Figure 5 – Material model law for the autoclaved aerated concrete**

The calculated tensile strength and fracture energy are in good conformity with the test results. The calculated modulus of elasticity  $E_{cal}$  is greater than the experimental secant modulus of elasticity  $E_S$  determined in the axial tensile tests, because the elastic deformations in the main cross-section in the bending tests are distinctly smaller than the deformations which form the basis of the calculation for the tensile modulus of elasticity  $E_S$  (see Table 2). The results show

that autoclaved aerated concrete is a little ductile material comparable to mortar (see characteristic length  $l_{ch}$ ).

#### (4) Adhesive tensile strength

The adhesive tensile strength between the mortar and the masonry unit was determined in axial tensile tests on autoclaved aerated concrete cylinders (diameter 100 mm) mortared with general purpose mortar (GPM) and a thin-layer mortar (TLM), respectively. Tests were made both on the adhesive tensile strength in the bed joints and in the head joints. In the tests with autoclaved aerated concrete and thin-layer mortar failure frequently occurred in the masonry unit. In the tests with general purpose mortar the post-peak behaviour could be determined with the test setup shown in Figure 6 (left). In Figure 6 (right) typical stress-crack width curves of the adhesive tensile strength tests between the head joint surfaces and general purpose mortar are presented. The fracture energies determined from this were taken into account in the Finite Element simulations of the wall tests.

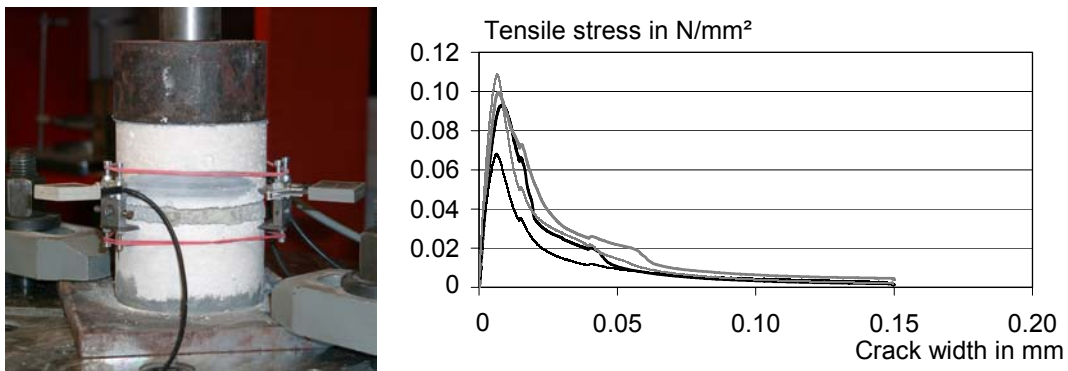


**Figure 6 – Adhesive tensile strength tests on test specimens of autoclaved aerated concrete with general purpose mortar**

The adhesive tensile strength values are summarized in Table 3.

**Table 3 – Bonding properties (axial adhesive tensile strength tests)**

|  | AAC / TLM  |           | AAC / GPM  |           |
|--|------------|-----------|------------|-----------|
|  | Head joint | Bed joint | Head joint | Bed joint |
| Adhesive tensile strength [N/mm <sup>2</sup> ] | ≥ 0.38     | 0.36      | 0.09       | 0.08      |

#### (5) Initial shear strength

Two methods are currently used in Germany for the determination of the initial shear strength – the initial shear strength test according to the German Standard DIN 18555-5 [12] and the European Standard DIN EN 1052-3 [13], respectively. The initial shear strengths determined according to the European test method are half of the values determined according to the German test method. Neither the test method according to [12] nor the test method according to [13] is suitable for the direct determination of the shear stress-displacement-curves due to the shear and axial stress distributions in the specimens, which were determined among other things with Finite Element Calculations [14]. In the research project carried out, the initial shear strength of the thin-layer mortar is determined exclusively with the method according to [12]. For the

general purpose mortar the initial shear strength was determined with both test methods. The difference determined already in earlier investigations between the two test methods has been approximately confirmed. The test according to [13] was made for the general purpose mortar in bond with the bed joint surface with four different loading levels normal to the bed joint, see Figure 7 (left). In the tests, deformations parallel and perpendicular to the bed joint were determined. The test results were simulated with the Finite-Element-Method from which the material laws were inversely determined for describing the bonding behaviour under shear stress. The comparison of the shear stress-displacement-curves measured in the middle of the overlap length with the Finite Element calculations is shown in Figure 7 (right). The essential test results of the initial shear stress tests are contained in Table 4.

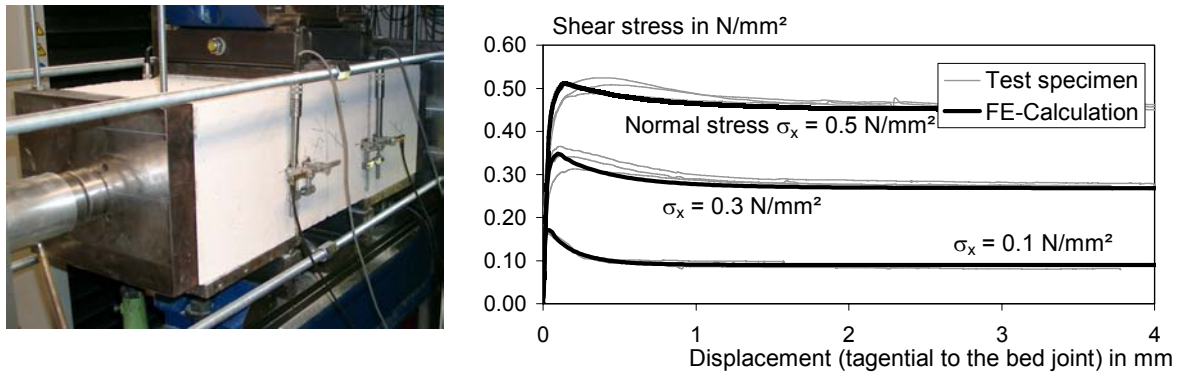


**Figure 7 – Initial shear stress tests according to /13/ and comparison between the experimental shear stress-displacement-curves and results from Finite Element Calculations**

**Table 4 – Bonding properties (initial shear stress tests)**

|                   |   | AAC / GPM        |                       | AAC / TLM  |           |   |
|-------------------|---|------------------|-----------------------|------------|-----------|---|
|                   |   | Head joint       | Bed joint             | Head joint | Bed joint |   |
| DIN 18 555-5      | Initial shear strength [N/mm <sup>2</sup> ] | -                | 0.15                  |            | 0.78      |   |
| EN 1052-3<br>/13/ | Initial shear strength [N/mm <sup>2</sup> ] | σ <sub>x</sub> = | 0                     | 0.14       | 0.08      | - |
|                   |   |                  | 0.1 N/mm <sup>2</sup> |            | 0.18      |   |
|                   |   |                  | 0.3 N/mm <sup>2</sup> |            | 0.34      |   |
|                   |   |                  | 0.5 N/mm <sup>2</sup> | -          | 0.51      |   |
|                   | Coefficient of static friction [-]          |                  | 0.82                  |            |           |   |
|                   | Coefficient of sliding friction [-]         |                  | 0.90                  |            |           |   |

### **THEORETICAL AND EXPERIMENTAL TESTS ON WALL TEST SPECIMENS**

In Germany, shear tests are carried out on storey-high, square masonry panels (see Figure 8 (left)) within the scope of tests on the general building inspection approval. The standardized test method has appeared to be suitable for determining the shear strength of masonry for many years, even if the test method is disputed to the extent that the load bearing capacity of the masonry is not determined, because the test walls are loaded differently than stiffening walls in buildings. The primary concern however, within the scope of this research project, was to test the load bearing behaviour of masonry walls with the most uniform possible shear stress and exactly defined boundary conditions.

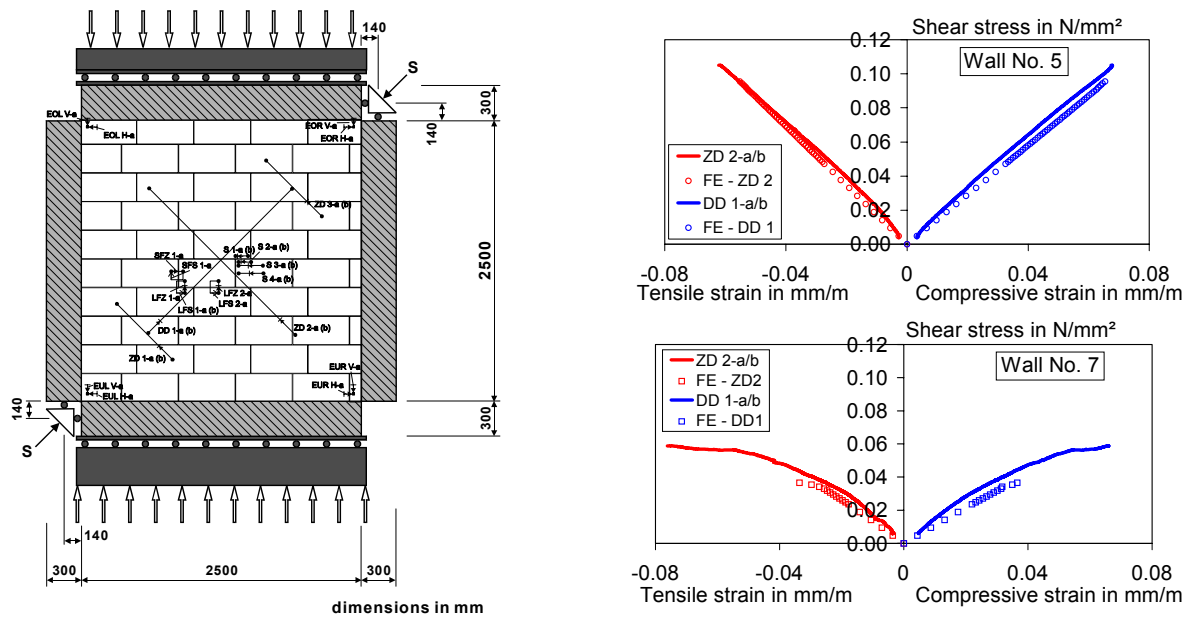


**Figure 8 – Test method and test specimen for the determination of the shear strength with measuring points (left), comparison of the experimental shear stress-strain-curves with results from Finite-Element-Calculations (right)**

With the test structure presented in Figure 8 (left), tests were carried out altogether on 8 different masonry walls. An overview of the test programme is given in Table 5.

**Table 5 – Results of wall tests compared to FE-Calculations**

| No. | Unit                                 | Mortar | Head joint | Overlap [mm] | Compressive stress [N/mm <sup>2</sup> ] | max $\tau$ [N/mm <sup>2</sup> ] |      |
|-----|--------------------------------------|--------|------------|--------------|---|---------------------------------|------|
|     |                                      |        |            |              |   | observed                        | FE   |
| 1   | Without perforations (Figure 1 left) | TLM    | filled     | 250          | 0                                       | 0.12                            | 0.10 |
| 2   |                                      |        | unfilled   |              |   | 0.14                            | 0.11 |
| 3   |                                      |        |            | 100          |   | 0.09                            | 0.10 |
| 4   |                                      |        | filled     | 250          |   | 1.1                             | 0.23 |
| 5   |                                      | GPM    | unfilled   |              | 0                                       | 0.11                            | 0.10 |
| 6   |                                      |        |            |              |   | 0.05                            | 0.05 |
| 7   |                                      |        |            | 100          |   | 0.06                            | 0.04 |
| 8   | With perforations (Figure 1 right)   | TLM    | unfilled   | 250          | 0                                       | 0.05                            | 1    |

1 not yet determined

A large number of deformation measurements were carried out on the test specimens in the masonry unit and joint area, in the direction of the main compressive and main tensile stresses in the masonry and also for determination of the displacements of the corner of the walls (Figure 8, left). The maximum shear strength is calculated from the diagonal force S introduced and the cross-sectional area  $A = 2500 \cdot 300 \text{ mm}^2$ :  $\max \tau = S / (1.41 \cdot A)$ . The experimentally determined shear strength values are given in Table 5 (observed max  $\tau$ ).



The shear tests were checked with the help of the Finite-Element-Method employing the material laws previously determined from the small test specimens. In the calculations the load introduction device (i. e. the concrete beam) was modelled as well, so that the Finite-Element-Model of the wall tests selected and the material laws determined from the small tests could be checked.

The calculated shear strength values are also given in Table 5 (FE max  $\tau$ ). Basically, the shear strength values determined by calculation are slightly lower than the experimental values. Only in the case of Wall No. 4, with a simultaneously acting vertical load, was there a significant difference between the Finite-Element-Calculations and the test value. Typical comparisons of the stress-strain-curves determined experimentally and by calculation (diagonal measuring points in the direction of the main stresses) of the test specimen No. 5 and No. 7 are presented in Figure 8 (right). The stress-strain-curves determined by calculation are in a good conformity in all cases with the test values. Figure 8 (right) shows that the calculated shear strength of wall No. 7 is relatively lower than the experimental determined value, but it has to be taken into account that just one wall each was tested. Figure 8 (right) shows further influences of the construction of the head joints (filled, unfilled) and the overlap on the shear strength and the curvature of the stress-strain-curves determined in the experimental test as well as in the numerical calculations. The analysis of the stress direction in the masonry showed that the formation of cracks normally begins in the corner units in the area of the load introduction, and after cracking, no definite bearing load increase is possible. In particular with high bonding strengths between the masonry unit and the mortar the load bearing capacity of the wall is decisively influenced by the strength of the corner units. The fact that the type of load introduction produces high stress concentrations in the corner units may also be the cause for the differences between the calculated and the experimentally determined shear strength values. In the Finite-Element-Calculations an optimum bond is assumed between the concrete beam and the masonry. Slight slipping – as is to be expected in the test – however, leads to a reduction in the stress peaks. The comparison of the experimental and calculated tests shows that with the Finite-Element-Model selected, and in particular the material laws determined in the small-scale tests, the wall tests can be simulated quite well.

In further numerical calculations, at present still in progress, the same masonry walls are modelled without modelling of the load introduction device (concrete beam): the load is applied instead by constant displacements to the masonry edges. The simulation of this “optimum” shear test will investigate to what extent the load introduction device influences the shear strength of the masonry. In the next step with this “optimum” shear test, a parametric study using different variables influencing the shear strengths will be carried out. On the basis of the results, it is intended to derive equations for the determination of the shear strength of masonry, which contain the essential geometrical characteristic values and building material values.

## **SUMMARY AND OUTLOOK**

In the research project carried out, a determination was first made of the material laws for masonry units and the bonding properties between masonry units and mortar in a large number of small specimen tests. In some cases the material laws or properties were determined inversely by Finite-Element-Calculation of the small specimen tests. The experimental tests carried out on storey-high, shear loaded masonry walls were simulated with the help of the

Finite-Element-Method and the application of these material laws. The results of the experimental tests and the calculations with the Finite-Element-Method are in quite good conformity. The calculations show that with the shear testing method as used in Germany, the shear strength of the masonry is considerably influenced by the load introduction process. By means of the simulation of an “optimum” shear test in parametric studies, the essential variables influencing the shear strength of the masonry will be characterized and simple calculation formulae will be derived on the basis of the numerical calculations.

## ACKNOWLEDGEMENT

The research project was kindly financially supported by the German Research Foundation.

## REFERENCES

1. DIN 1053-1 11.96. Mauerwerk; Berechnung und Ausführung. 1996.
2. DIN V ENV 1996-1-1. Bemessung und Konstruktion von Mauerwerksbauten - Regeln für bewehrtes und unbewehrtes Mauerwerk. 1996.
3. Mann, W., Müller, H. Bruchkriterien für querkraftbeanspruchtes Mauerwerk und ihre Anwendung auf gemauerte Windscheiben. In: Bautechnik (1973), Nr. 12, S. 421-425. 1973.
4. Mann, W., Müller, H. Schubtragfähigkeit von Mauerwerk. Berlin: Ernst & Sohn. - In: Mauerwerk-Kalender 3 (1978), S. 35-65. 1978.
5. Mann, W. ; Müller, H. Cracking Characteristics of Transversely Loaded Brick Masonry in Theory and Practice. In: Proceedings of the Fifth International Brick Masonry Conference, Washington, October 5-10, 1979, (Wintz, J.A. ; Yorkdale, A.H. (Ed.)), S. 239-246. McLean, Virginia : Brick Institute of America, 1982.
6. Mann, W., Müller, H. Nachrechnung der Wandversuche mit einem erweiterten Schubbruchmodell unter Berücksichtigung der Spannungen in den Stoßfugen. Anlage 2 zum Forschungsbericht „Untersuchungen zum Tragverhalten von Mauerwerksbauten unter Erdbebeneinwirkung“, Forschungsbericht IV/1-5-488/86, Darmstadt. 1986.
7. Schneider, K. H., Wiegand, E., Jucht, K.-D. Innerer Spannungszustand bei Mauerwerk mit nicht vermörtelten Stoßfugen. Bauforschungsbericht des Bundesministeriums für Raumordnung, Bauwesen und Städtebau F 1360. Stuttgart: IRB Verlag. 1976.
8. Graubner, C.-A., Simon, E. Zur Schubtragfähigkeit von Mauerwerk aus großformatigen Steinen. Berlin : Ernst & Sohn. - In: Mauerwerk-Kalender 26 (2001), S. 7-88. 2001
9. Simon, E. Schubtragverhalten von Mauerwerk aus großformatigen Steinen. Darmstadt, Technische Universität, Fachbereich Bauingenieurwesen und Geodäsie, Dissertation, 2002.
10. Graubner, C.-A., Kranzler, T., Schubert, P., Simon, E. Festigkeitseigenschaften von Mauerwerk - Teil 3: Schubfestigkeit von Mauerwerksscheiben. Berlin : Ernst & Sohn. - In: Mauerwerk-Kalender 30 (2005), S. 7-88. 2005
11. DIN V 4165(Vornorm), Ausgabe:2003-06. Porenbetonsteine – Plansteine und Planelemente. 2003.
12. DIN 18 555-5 03.86. Prüfung von Mörteln mit mineralischen Bindemitteln; Festmörteln; Bestimmung der Haftscherfestigkeit von Mauermörteln. 1986.
13. DIN EN 1052-3/A1 (Norm-Entwurf), Ausgabe: 2005-02. Prüfverfahren für Mauerwerk - Teil 3: Bestimmung der Anfangsscherfestigkeit (Haftscherfestigkeit); Deutsche Fassung EN 1052-3:2002/prA1:2004
14. Roßbach, M., Schmidt, U., Schubert, P. Untersuchungen zur Schubtragfähigkeit von Ziegelmauerwerk. In: Mauerwerk 8 (2004), Nr. 2, S. 72-81